Evaluation of Edge Electron Temperature Fluctuation by the Use of Fast Voltage Scanning Method on TST-2*)

Yoshihiko NAGASHIMA, Akira EJIRI, Yuichi TAKASE, Masateru SONEHARA, Hidetoshi KAKUDA, Takuya OOSAKO[1)], Junichi HIRATSUKA, Osamu WATANABE, Takashi YAMAGUCHI, Hiroaki KOBAYASHI, Takuma WAKATSUKI, Takuya SAKAMOTO, Kentaro HANASHIMA, Takanori AMBO, Ryota SHINO and Shigeru INAGAKI[2)]

The University of Tokyo, Chiba 277-8561, Japan
[1)]*CEA, Saint Paul Lez Durance 13108, France*
[2)]*Kyushu University, Kasuga 816-8580, Japan*

(Received 5 December 2010 / Accepted 2 February 2011)

Edge electron temperature fluctuation is evaluated by the use of fast voltage sweeping technique on TST-2. The validity of obtained current-voltage characteristic curve was checked by comparing the time evolutions of floating potential between that obtained from the fast voltage sweeping technique and that measured with floating probe method. Good agreement between them was confirmed. We also found that fitting errors in the evaluation of the electron temperature itself are less than 10% of fluctuation levels of the electron temperature. Therefore the accuracy of the technique is applicable to study of plasma fluctuations.

Keywords: plasma turbulence, temperature fluctuation, edge plasma

DOI: 10.1585/pfr.6.2402036

1. Introduction

Development of fast, fine and precise electron temperature measurement technique in edge plasmas is important for fusion plasma research. In particular, transport caused by temperature gradient driven turbulence (i.e., ion temperature gradient turbulence) is believed to be significant in high performance fusion plasmas. There are many previous work on the electron temperature fluctuation with combination of Langmuir probes and complicated circuits [1–7]. In this paper, we propose an approach to estimate the turbulent electron temperature fluctuation in the TST-2 spherical tokamak [8]. The approach focuses on fast voltage sweep method applied to a single Langmuir probe to maintain fine spatial resolution; a triple probe technique was not used. Unlike the previous work, the circuit used in this experiment is simple, and is not a novel technique. Instead, we have tested validity of the method by comparing fluctuations measured with two different methods. Here we show preliminary waveforms of plasma fluctuations (fluctuations of electron temperature $\tilde{T}_e$, electron density $\tilde{n}_e$, and plasma potential $\tilde{\Phi}_p$) measured with the fast voltage sweep method. In addition, the comparison of the floating potential fluctuations ($\tilde{\Phi}_f$) between measured with the fast voltage sweep method and measured with the floating probe method to confirm that the fast voltage sweep method used in this experiment is valid. The comparison is a novel point in this paper. First, we describe the experimental setup in TST-2. Second, we give an example of preprocessing of probe current data before fitting them to a model I-V function. Third, we show an example of fitting procedure of the I-V data to the model. Finally, we compare $\tilde{\Phi}_f$s measured with the two methods, and discuss the results.

2. Experimental Setup

TST-2 is a small spherical tokamak device with major radius $R_0 \sim 0.38$ m, minor radius $a \sim 0.25$ m (aspect ratio $A \geq 1.5$), elongation $\kappa \leq 1.2$-1.8, and toroidal magnetic field $B_t \leq 0.3$ T. Typical plasma parameters are: plasma current $I_p \leq 200$ kA, line-averaged electron density $\overline{n}_e \leq 2 \times 10^{19}$ m^{-3}, and electron temperature at plasma center $T_{e,0} = 100$-300 eV. There are two kinds of operation in TST-2: One is ohmically heated discharge with/without auxiliary rf heatings at the ion cyclotron (21 MHz) and lower-hybrid (200 MHz) range of frequency [9, 10]. The other is electron cyclotron heating (ECH) discharge [11]. Plasmas in this experiment are produced by ohmic heating without rf injection. The low-field side boundary of the plasmas is determined by the limiter ($R = 0.63$ m) attached to the rf antenna.

Experimental data were obtained by a multi-channel Langmuir probe (LP) [12]. The LP is located at a toroidal angle of $\phi = -165°$ relative to the toroidal location of the rf antenna, and is radially movable. Figure 1 (a) shows photograph of the head of the LP and assignment of the elec-

author's e-mail: nagashima@k.u-tokyo.ac.jp
*) This article is based on the presentation at the 20th International Toki Conference (ITC20).

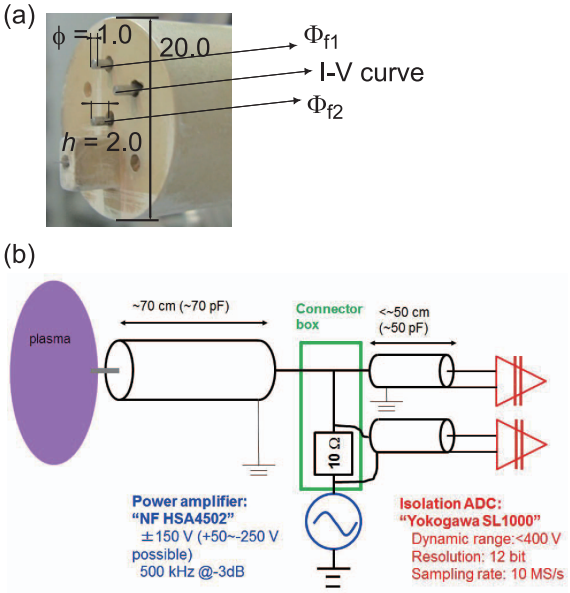

Fig. 1 (a) Photograph of Langmuir probe and usage of electrodes. (b) Schematic of data acquisition circuit.

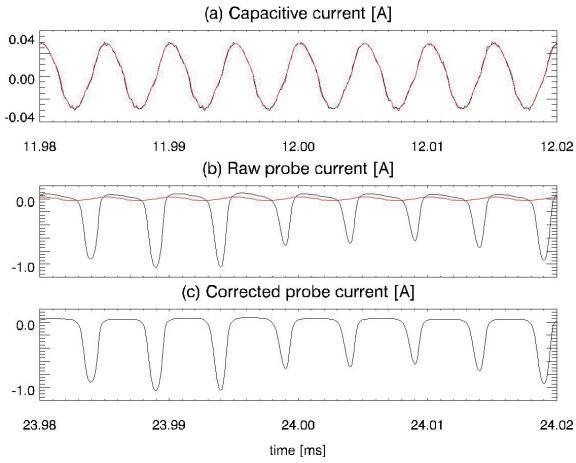

Fig. 2 Preprocessing of waveforms before I-V curve fitting procedure. (a) Waveform of raw probe current before plasma discharge (black), and estimation of capacitive current from derivative of sweep voltage at the same period (red). (b) Waveform of raw probe current during plasma discharge (black), and estimation of capacitive current from derivative of sweep voltage waveform at the same period (red). (c) Waveform of the corrected probe current subtracted by the estimated capacitive current (preprocessing). In (c), asymmetry of the probe current between at $dV/dt > 0$ and at $dV/dt < 0$ seen in (b) disappears in the preprocessed waveform in (c).

trode usage for the experiment. We use three electrodes. One electrode is used to obtain I-V curves by applying a sweeping sinusoidal bias voltage at 200 kHz, from which the local electron temperature T_e can be derived. Power spectrum of edge turbulent fluctuations observed on TST-2 has a maximum at a few tens kHz with the same order of frequency bandwidth. Therefore, the sweep frequency of 200 kHz is sufficient to measure the edge turbulence on TST-2. The other two electrodes measure the floating potentials (Φ_f) by floating probe technique. By the use of the two Φ_f data, we calculate the interpolated Φ_f ($\Phi_{f,i}$) at the location where the I-V curves are measured to be temporally compared with Φ_f measured with the fast voltage sweeping method. We set the radial location of the LP at $r = -20$ mm, where r represents the radial location relative to the low-field side limiter, and positive and negative r indicate outside and inside the limiter location. Duration time of plasmas in this experiment is about 20 ms, and we selected data for analysis when the low-field side of the plasma was bound by the limiter (20-30 ms).

Acquisition of reliable I-V curves is a key issue to obtain T_e fluctuation. When large bias voltage is applied to probe electrical circuit at high sweeping frequency, large capacitive current passes through the cable capacitance, and significantly distorts the raw probe current data from plasmas. On the contrary, the sheath capacitance is an order of 1 pF and is negligible. In previous work, combination of dummy probes and differential amplifiers has been used to subtract the capacitive current from the raw probe data. To avoid complexity of circuits, we don't use combination of the dummy probe and differential amplifier in this experiment. Instead, diagnostic systems are assembled close to each other to minimize length of the cable drive and the capacitive current (Fig. 1 (b)). The electrode is directly connected to coaxial cable with the length of ~ 70 cm (cable capacitance ~ 70 pF) leading to coaxial vacuum feedthrough. The outer conductor is connected to the vessel ground at the feedthrough (the connection is controllable). The small connector box including a shunt resister (~ 10 Ω) for the probe current measurement is directly connected to the feedthrough. The fast sweep voltage is supplied to the connector box through coaxial cables with the length of less than 50 cm. The power amplifier as voltage supplier is HSA4052 (manufactured by NF corporation, Japan), which can supply voltage of −250 to +50 V (2 A rms) swept at 500 kHz (−6 dB). We measure the probe current at the shunt resister and the voltage at the exit of the vacuum feedthrough by using an Analog-Digital Converter (SL1000 manufactured by Yokogawa Meter and Instruments Inc., Japan) through both cable drives of less than 50 cm. The ADC has 16 channels, and can measure voltage up to 400 V with the analog bandwidth up to 3 MHz. The maximum sampling rate is 10 MHz, thus, number of data points at an I-V curve is 25. Channels of the ADC are electrically isolated from one another, and resolution of voltage (dynamic range) is easily tunable in each channel. Therefore, we can directly measure large amplitude swept voltage signals and small amplitude current waveforms at the same sampling clock. In addition, the independent floating potentials (Φ_{f1} and Φ_{f2}) can be measured by the ADC simultaneously.

3. Data Analysis Procedure

Superposition of the capacitive current on the probe

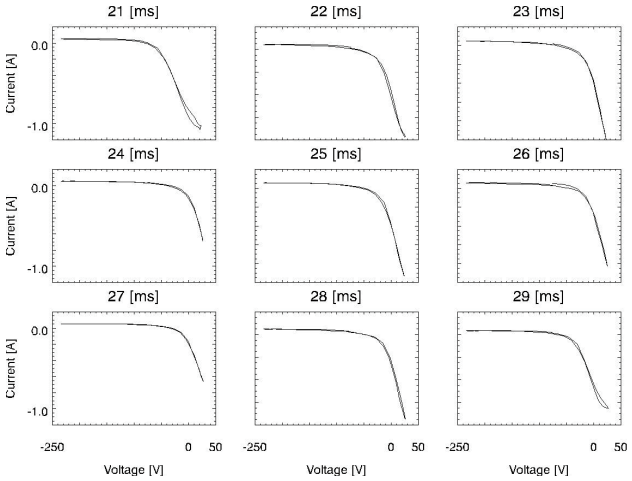

Fig. 3 I-V characteristic curves at different 9 periods (regular 1 ms intervals). In each plot, contiguous two I-V curves at $dI/dt > 0$ and at $dI/dt < 0$ during a sinusoidal cycle of voltage sweep are overploted. Hysteresis, asymmetry of I-V curves between at $dI/dt > 0$ and at $dI/dt < 0$, is not observed at any time. This indicates that the asymmetry is originated from temporal variation of plasmas.

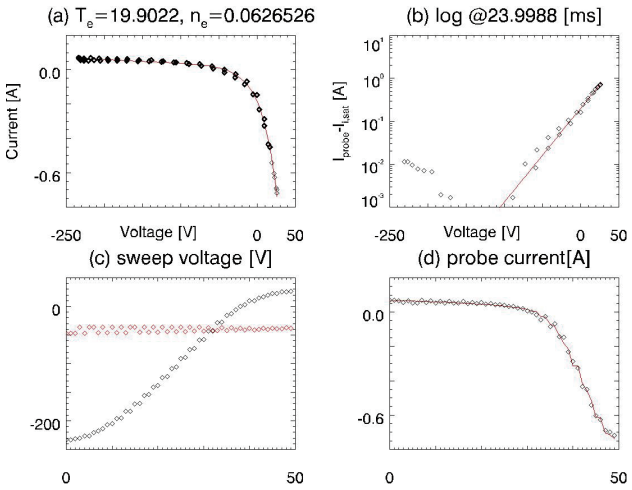

Fig. 4 Example of I-V curve measured at ~ 24 ms. (a) Linear plot of an I-V curve. Thick and thin black diamonds indicate data points used in the fitting procedure and all data points, respectively. We use data points $V < \Phi_f + 2T_e$ in the fitting procedure. Red line means fitted curve. Here, T_e of 20.0 ± 0.14 eV and n_e of 0.63 ± 0.035 × 10^{18} m^{-3} are obtained. (b) Logarithmic plot of the I-V curve at the same period as that in (a). In (b), current data is subtracted by ion saturation current. Electron deceleration range looks like consistent with the fitted curve. (c) Voltage data points (black) and temporal variation of $\Phi_{f,i}$ measured simultaneously (red). The temporal variation is included in errors of the fitting procedure. (d) Current data (black) and the fitted current (red).

current from plasmas is not negligible nevertheless the effort to minimize the cable capacitance. The superposition causes hysteresis of I-V curves, leading significant errors in evaluation of T_e. Therefore, next we perform preprocessing of the raw current data before calculating T_e by the fitting procedure. We estimate the capacitive current from derivatives of the voltage data, and the estimated capacitive current is subtracted from the raw probe current. Validity of the estimated capacitive current is checked by comparison with the raw probe current before plasma production (no current from plasmas). The preprocessing is shown in Fig. 2. Figure 2 (a) shows the comparison between the estimated capacitive current (red) and the raw probe current (black) before plasma production. Plasma current starts up at about 15 ms in typical TST-2 operations. Good agreement between the two waveforms is observed, and validity of the estimation is responsible to application of the estimation to the subtraction of the estimated capacitive current from the raw probe current. The subtraction is demonstrated in Figs. 2 (b, c). In Fig. 2 (b), the raw probe current (black) shows clear asymmetry between at $dI/dt > 0$ and at $dI/dt < 0$, and the estimated capacitive current (red) is not negligible relative to the raw probe current. However, the asymmetry may drastically vanish after the subtraction, shown in Fig. 2 (c). The hysteresis mainly caused by the asymmetry is checked in a number of period, shown in Fig. 3 (9 periods at regular 1 ms intervals). The hysteresis is sometimes observed, however, is not at any time. The asymmetry constantly occurs when the subtraction is incomplete and/or the ion polarization drift current is not negligible. Therefore, the negligible asymmetry demonstrates that the subtraction looks like work well.

After the preprocessing, another key issue to obtain T_e is the fitting procedure that the obtained I-V curve is fitted to the model I-V curve within some errors. Then, T_e, electron density n_e, Φ_f, and plasma potential Φ_p are derived from the fitted I-V curve. The model I-V curve is chosen as,

$$I = I_{i,sat}(V_{probe}) + I_{e,sat} \exp\Big(\frac{V_{probe} - \Phi_{plasma}}{T_e}\Big), \quad (1)$$

$$I_{i,sat}(V_{probe}) = I_{i,sat,0}(1 - aV_{probe}), \quad (2)$$

where $I_{i,sat}(V_{probe})$ is an indicator of the ion saturation current, $I_{e,sat}$ is the electron saturation current, V_{probe} is the voltage applied to the electrode, Φ_{plasma} is the plasma potential, T_e is the electron temperature [eV], and a is a coefficient representing dependence of the ion saturation current range on the applied voltage. The voltage is based on the vessel ground. The dependence of the ion saturation current range on the applied voltage may be originated from the finite size of sheath surface of the electrode used, and we often obtain reliable fitted result by including the dependence. Here, the ion saturation current $I_{i,sat}$ is defined as $I_{i,sat}(V_{probe} = \Phi_f)$ to obtain n_e, and $\Phi_{plasma} = \Phi_f + 2.94T_e$ considering that the deuteron mass and difference of particle collection area between electrons and ions.

An example of the fitting procedure is shown in Fig. 4. I-V curves are obtained at 400 kHz (sweep frequency is 200 kHz) with the sampling rate of 10 MHz, then we have 25 data points per an I-V curve. In the case, amount of data points in the electron deceleration range is typically a few

and several points. Therefore, we combine two contiguous I-V curves to compensate small amount of data points in the electron deceleration range, leading to decrease of error in evaluation of T_e. There are mainly two error sources in evaluation of T_e from the fitting procedure. One is variance of data in the fitting procedure itself, and the other is variance in selecting data range used in the fitting procedure. The former error includes effect of the temporal variation of plasma parameters, and reflects variance in the fitting procedure. The latter error is complicated. When we choose the fitting range in the vicinity of Φ_f, T_e tends to be higher than T_e obtained from the range including the electron deceleration area. A candidate for the reason is distortion of electron distribution function in high energy part by the electron tail. On the contrary, when the fitting range is close to the electron saturation current, the evaluated T_e also tends to be high because of discrepancy between the model and the data used in fitting. In this analysis, we choose the fixed fitting range of $V_{probe} < \Phi_f + \sim 2T_e$ under which we typically obtain the minimum variance between Φ_f observed by the fitting procedure and $\Phi_{f,i}$. In addition, we observed the minimum T_e during scan of the fitting range in the fitting procedure using the same data set. It should be noted that the fitting range is fixed in the fitting procedure of this paper.

4. Preliminary Waveforms of Plasma Quantity Derived from the Fitting Procedure

Using the fitting procedure, we obtained preliminary waveforms that are required to estimate fluctuations. In addition, we compare Φ_f measured with the two methods to confirm the validity of the fitting procedure. Figures 5 (a-e) show waveforms obtained from the fitting procedure as well as plasma toroidal current (Fig. 5 (f)). In Figs. 5 (a, b), T_e and density in black are obtained much higher than their errors in red. Fluctuation levels of T_e ~10% are smaller than those of n_e > 20%. The errors of T_e and n_e are less than 1% and 5%, respectively. Figure 5 (c) demonstrates the comparison of Φ_fs measured with the I-V curves (black) and with the floating probe method (red) during whole of discharge duration. The T_e fluctuation observed here is small relative to the $\tilde{\Phi}_f$, therefore, Φ_p fluctuation, shown in Fig. 5 (d), seems to be dominated by $\tilde{\Phi}_f$. Enlarged view of Fig. 5 (c) in the vicinity of 24 ms is shown in Fig. 5 (e), and good agreement between them is observed. This agreement confirms that the fitting procedure works well in the case.

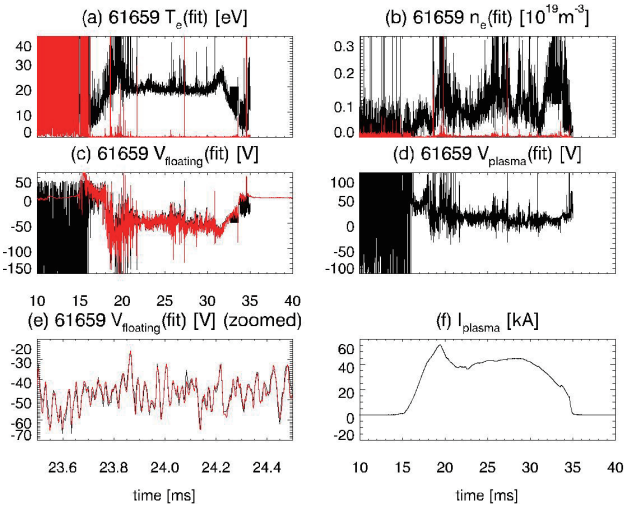

Fig. 5 Waveforms derived by results from fast voltage sweep method. Plots in black indicate fitted parameters. (a) T_e, (b) n_e, (c) Φ_f, (d) Φ_p, and (e) enlarged view of the Φ_f. (f) Discharge plasma current. In (a) and (b), plots in red indicate errors in fitting. In (c) and (e), plots in red indicate $\Phi_{f,i}$s derived from Φ_{f1} and Φ_{f2}. In (e), good agreement between the fitted Φ_f and $\Phi_{f,i}$ is observed.

We have evaluated quantitatively the fluctuations of the electron temperature and plasma potential in a case. Standard deviations of T_e, Φ_f, and Φ_p during 22-25 ms in Fig. 5 are 1.4 eV, 8.0 V, and 7.9 V, respectively. The variance of Φ_p, σ^2_{plasma} can be written as,

$$\langle\sigma^2_{plasma}\rangle = \langle(\sigma_{float} + 2.9\sigma_{temp})^2\rangle \sim \langle\sigma^2_{float}\rangle + 5.9\langle\sigma_{float}\sigma_{temp}\rangle + 8.6\langle\sigma^2_{temp}\rangle, \quad (3)$$

where $\langle\ \rangle$ indicates ensemble average, σ^2_{float} and σ^2_{temp} are the variances of the floating potential and electron temperature, and $\sigma_{float}\sigma_{temp}$ is the covariance between the floating potential and electron temperature, respectively. A Result of σ^2_{float} (64.0) ~ σ^2_{plasma} (62.0) was obtained. A possible reason for the result is that summation of the second and third terms is much smaller than the first term on the right-hand side in this case.

For future work, a few problems should be resolved. First, the fitting procedure fails in some periods in a discharge, therefore, stability of convergence of the fitting procedure should be improved. Next, accuracy of $\Phi_{f,i}$ should be confirmed. When we focus on the minimum variance between Φ_f measured with the fitting procedure and $\Phi_{f,i}$ in evaluation of T_e, values of T_e are also affected by the target $\Phi_{f,i}$. The most relevant procedure should be found. Finally, the results that $\sigma^2_{float} \sim \sigma^2_{plasma}$ should be tested in detail. In previous work, the relationship that $\sigma^2_{float} \sim \sigma^2_{plasma}$ is not the universal result, but may be a specific result in the case.

5. Summary and Discussion

In summary, by the use of conventional fast voltage sweep technique, we have evaluated fast waveforms of T_e in the edge plasma of the TST-2 spherical tokamak. The novelty of this paper is comparison of Φ_fs measured with the two methods, and good agreement between them is observed. We also found that fitting errors in the evaluation of the electron temperature itself are less than 10% of fluctuation levels of the electron temperature. Therefore the

accuracy of the technique is applicable to study of plasma fluctuations.

Acknowledgment

This work was supported by Japan Society for the Promotion of Science (JSPS) Grants-in-Aid for Scientific Research (S) No. 21226021 and for Scientific Research (A) No. 21246137.

[1] C. Hidalgo, R. Balbín, M. Pedrosa, I. García-Cortés and M. Ochando, Phys. Rev. Lett. **69**, 1205 (1992).
[2] L. Giannone, R. Balbfn, H. Niedermeyer, M. Endler, G. Herre, C. Hidalgo, A. Rudyj, G. Theimer, P. Verplanke and the W7-AS Team, Phys. Plasmas **1**, 3614 (1994).
[3] M. Meier, R. Bengtson, G. Hallock and A. Wooton, Phys. Rev. Lett. **87**, 085003 (2001).
[4] M. Schubert, M. Endler, H. Thomsen and T. W.-A. Team, Rev. Sci. Instrum. **78**, 053505 (2007).
[5] H. Müller, J. Adamek, J. Horacek, C. Ionita, F. Mehlmann, V. Rohde, R. Schrittwieser and the ASDEX Upgrade Team, Contrib. Plasma Phys. **50**, 847 (2010).
[6] J. Boedo, D. Gray, R.W. Conn, P. Luong, M. Schaffer, R. Ivanov, A. Chernilevsky, G.V. Oost and T.T. Team, Rev. Sci. Instrum. **70**, 2997 (1999).
[7] J. Boedo, D. Rudakov, R. Moyer, G. McKee, R. Colchin *et al*., Phys. Plasmas **10**, 1670 (2003).
[8] Y. Takase, A. Ejiri, N. Kasuya, T. Mashiko, S. Shiraiwa *et al.*, Nucl. Fusion **41**, 1543 (2001).
[9] T. Oosako, Y. Takase, A. Ejiri, Y. Nagashima, Y. Adachi *et al.*, Nucl. Fusion **49**, 065020 (2009).
[10] Y. Nagashima, T. Oosako, Y. Takase, A. Ejiri, O. Watanabe *et al.*, Phys. Rev. Lett. **104**, 045002 (2010).
[11] A. Ejiri, Y. Takase, T. Oosako, T. Yamaguchi, Y. Adachi *et al.*, Nucl. Fusion **49**, 065010 (2009).
[12] K. Yamada, Master's thesis (2009).